

# A Structured Catalyst toward Mercaptan Sweetening with Largely Enhanced Synergistic Effect

Zhiyong Sun,<sup>†,‡</sup> Lan Jin,<sup>†</sup> Yufei Zhao,<sup>†</sup> Shan He,<sup>†</sup> Shuangde Li,<sup>†</sup> Min Wei,<sup>\*,†</sup> and Liren Wang<sup>\*,†</sup>

<sup>†</sup>State Key Laboratory of Chemical Resource Engineering, Beijing University of Chemical Technology, Beijing 100029, P. R. China

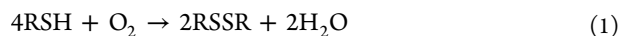
<sup>‡</sup>Science and Technology on Marine Corrosion and Protection Laboratory, Luoyang Ship Material Research Institute, Qingdao 266101, P. R. China

**S** Supporting Information

**ABSTRACT:** A structured catalyst has been fabricated by immobilizing cobalt phthalocyanine tetrasulfonate (CoPcS) on a MgNiAl mixed metal oxide (MgNiAl-MMO) film derived from calcination of layered double hydroxide (LDH). The resulting CoPcS/MgNiAl-MMO catalyst exhibits excellent activity, stability, and recyclability for the reaction of mercaptan sweetening. SEM images show that the structured catalyst is composed of thin MMO nanoflakes perpendicular to the Al substrate. The synergistic effect between the oxidation center (CoPcS) and the abundant moderate basic sites on the surface of the MgNiAl-MMO substrate plays an important role in the sweetening process, accounting for the largely enhanced catalytic behavior (conversion: 92.8%; selectivity: 100%). In addition, the structured catalyst exhibits superior catalysis regeneration performance, owing to its specific architecture and strong mechanical stability. This work demonstrates a facile approach for modulating the synergistic effect between the active center and the basicity for the structured catalyst, for the purpose of achieving largely enhanced catalytic behavior in the petroleum refining industry.

## 1. INTRODUCTION

Mercaptans (RSH) present in petroleum products, even in very small quantities, give rise to a foul odor which seriously harms human health and the atmospheric environment.<sup>1</sup> It is therefore necessary to remove them from petroleum products (usually referred to as “sweetening”).<sup>2,3</sup> In the petroleum refining industry, the most commonly practiced method is the Merox process of sweetening, which involves catalytic oxidation of mercaptans to innocuous disulfides with air by cobalt phthalocyanine (CoPc) or its derivatives in the presence of caustic soda as cocatalyst.<sup>4</sup> The oxidation reaction is as follows:<sup>5</sup>



To date, caustic soda solution is most widely used in the industrial Merox process to eliminate mercaptans from petroleum products. However, caustic soda has been recognized as a hazardous waste in this process, which leads to water pollution and destruction of the ecological environment. Moreover, the disposal of the spent caustic liquor is becoming more difficult and expensive due to the steady tightening of environmental regulations worldwide.<sup>6</sup> Therefore, extensive studies have been conducted on the substitution of caustic soda by solid bases so as to develop a more environmentally friendly and effluent-free process for mercaptan sweetening.

Mixed metal oxides (denoted as MMO) derived from thermal decomposition of layered double hydroxide materials (LDHs)<sup>7–13</sup> have been regarded as promising solid bases with controllable basicity via changing their chemical composition, preparation method, and thermal treatment conditions (calcination temperature).<sup>14–18</sup> For instance, Valente et al.<sup>19</sup> prepared various bimetallic oxides (MgAl, NiAl, and ZnAl, etc.) with different basicities by calcination of the corresponding

LDH precursors. In addition, the basicity of MgAl MMO varies with the calcination temperature<sup>20</sup> or modification by fluoride anion.<sup>21</sup> However, the basicity of a bimetal oxide is difficult to adjust very precisely, which is a main obstacle for the design and tuning of solid base-based catalysts. Therefore, trimetallic or multimetallic oxides, with a facile tuning of basicity by changing the metallic composition and relative content, would provide a highly desirable approach for achieving this goal.

It has been reported that MgAl-MMO-supported cobalt phthalocyanine (CoPc) powdered catalysts, which include oxidation site (Co<sup>2+</sup>) and basic site (MgAl-MMO) with cooperative interaction, can effectively oxidize mercaptans to disulfides.<sup>22</sup> In our previous work,<sup>23</sup> a structured catalyst was fabricated by immobilizing cobalt phthalocyanine tetrasulfonate (CoPcS) on MgAl-MMO film, which exhibits high activity, stability, and recyclability for mercaptan sweetening. Despite all the progress, the uncontrollability of basicity and number of basic sites restricts a further improvement of catalytic activity. Therefore, this inspired us to fabricate a structured catalyst by the immobilization of CoPcS onto multimetallic oxides with tunable basicity, for the purpose of enhancing the synergistic effect between active center and basicity to the maximal extent.

In this work, we report the preparation of structured catalysts based on cobalt phthalocyanine tetrasulfonate (CoPcS) supported on MgNiAl-MMO film resulting from calcination of the LDH precursor, which was used for the mercaptan sweetening process via the oxidation of 1-octanethiol to the corresponding disulfide as a model reaction. SEM images show

**Received:** December 19, 2013

**Revised:** March 2, 2014

**Accepted:** March 4, 2014

**Published:** March 4, 2014

that the structured catalyst is composed of thin MMO nanoflakes perpendicular to the Al substrate, with a specific surface area of 97.7 m<sup>2</sup>/g and a pore size distribution of 10–100 nm determined by BET measurements. The basicity and the number of moderate basic sites for the CoPcS/MgNiAl-MMO structured catalyst can be tuned conveniently by changing the relative content of Mg and Ni. A largely enhanced catalytic activity with a conversion as high as 92.8% was obtained owing to the promoted synergistic effect between oxidation center (CoPcS) and the moderate basic site. Therefore, this work provides a facile method for the fabrication of structured catalyst with largely enhanced activity and stability, which can be potentially applied as an eco-friendly catalyst for sweetening in the petroleum refining industry.

## 2. EXPERIMENTAL SECTION

**2.1. Materials.** Tetrasodium salt of cobalt(II) 4',4'',4''',4''''-tetrasulfophthalocyanine (Co(II)Pc(SO<sub>3</sub>Na)<sub>4</sub>, denoted as CoPcS) and 1-octanethiol (purity >97%) were provided by J&K Chemical Ltd. The pure aluminum substrate (purity: >99.99%; thickness: 0.2 mm) was purchased from Beijing General Research Institute for Non-Ferrous Metals. The chemicals including ethanol, NaOH, (NH<sub>2</sub>)<sub>2</sub>CO, Mg(NO<sub>3</sub>)<sub>2</sub>·6H<sub>2</sub>O, and Ni(NO<sub>3</sub>)<sub>2</sub>·6H<sub>2</sub>O are of analytical grade and were used without further purification. Deionized water was used in all the experimental processes.

**2.2. Fabrication of the Structured Catalysts.** The MgNiAl-LDH films were prepared by an in situ crystallization on the pure aluminum substrate. The substrate was cleaned with acetone, ethanol, and deionized water in sequence before use. In a typical procedure, 0.032 mol of Mg(NO<sub>3</sub>)<sub>2</sub>·6H<sub>2</sub>O and 0.194 mol of (NH<sub>2</sub>)<sub>2</sub>CO were dissolved in deionized water to form a clear solution with a total volume of 600 mL (denoted as solution I). Solution II was prepared by dissolving Mg(NO<sub>3</sub>)<sub>2</sub>·6H<sub>2</sub>O (*a* mol), Ni(NO<sub>3</sub>)<sub>2</sub>·6H<sub>2</sub>O (*b* mol in which *a* + *b* = 0.032 mol, *a*/*b* = 10, 15, 20, 25, 30, and 40, respectively), and 0.194 mol of (NH<sub>2</sub>)<sub>2</sub>CO in deionized water with a total volume of 600 mL. The Al substrate (28 cm × 15 cm) was rolled into tubular shape and immersed vertically in solution I, which was heated at 70 °C for 24 h. Afterward, the substrate was withdrawn from solution I and immersed into solution II with various Mg/Ni ratio at 70 °C for 24 h. The substrate was then withdrawn, rinsed with deionized water, and dried at room temperature. Subsequently, the as-prepared MgNiAl-LDH films were heated at 500 °C for 4 h (heating rate: 2 °C/min) to obtain the MgNiAl-MMO films with a different Mg/Ni ratio.

The structured catalysts were prepared by immersing fresh MMO film into anhydrous methanol solution containing Co(II)Pc(SO<sub>3</sub>Na)<sub>4</sub> at various concentrations (10, 20, 30, and 40 ppm, respectively) with dry N<sub>2</sub> flow at 25 °C for 1 h, followed by drying under vacuum at 50 °C for 2 h. The resulting structured catalysts (denoted as CoPcS/MgNiAl-MMO) typically contain 0.79–1.27 mg CoPcS per 140 cm<sup>2</sup> substrate in this work (Figure S1, Supporting Information). Two comparison film samples, CoPcS/NiAl-MMO and CoPcS/Al were prepared by a similar procedure. A powdered sample of CoPcS/MgNiAl-MMO was prepared according to the reported method.<sup>22</sup> Before use, all these catalyst samples were stored free of moisture and air.

**2.3. Catalytic Oxidation of Mercaptan.** The catalytic properties of the catalysts were tested in the oxidation reaction of 1-octanethiol, which was performed in a thermostatted

double-walled glass flask equipped with a high-speed stirrer.<sup>22</sup> The structured catalyst (with a substrate area of 140 cm<sup>2</sup>) was rolled into a cylinder and placed into the reaction flask. After the injection of 1.40 mL of 1-octanethiol (containing 1000 ppm mercaptan sulfur in the synthetic feed), the reaction occurred at 25 °C under constant oxygen pressure (1.0 atm). The catalytic behavior of powdered catalysts containing the same content of CoPcS was evaluated under the same conditions. The reaction products were analyzed by GC–MS, and it was found that the disulfide (C<sub>8</sub>H<sub>17</sub>SSC<sub>8</sub>H<sub>17</sub>) was the only product, indicating a 100% of selectivity. No H<sub>2</sub>O<sub>2</sub> accumulation was detected. Therefore, the conversion of 1-octanethiol proceeds according to the following equation: 4C<sub>8</sub>H<sub>17</sub>SH + O<sub>2</sub> → 2C<sub>8</sub>H<sub>17</sub>SSC<sub>8</sub>H<sub>17</sub> + 2H<sub>2</sub>O. The lifetime test of the catalyst was performed by withdrawing the structured catalyst from one reaction vessel and installing it into another vessel with new reactants, followed by the operation above.

**2.4. Techniques of Characterization.** X-ray diffraction (XRD) patterns of samples were obtained on a Shimadzu XRD-6000 diffractometer, using Cu K $\alpha$  radiation ( $\lambda$  = 0.154 nm) at 40 kV, 30 mA, a scanning rate of 5°/min, a step size of 0.02°/s, and a 2 $\theta$  angle ranging from 3° to 70°. The morphology and the thickness of the films were investigated by using a scanning electron microscope (Zeiss Supra 55) combined with energy-dispersive X-ray spectroscopy (EDS) for the determination of metal composition. The accelerating voltage applied was 20 kV. All samples were sputtered with platinum. Transmission electron microscopy (TEM) images were obtained using a JEOL JEM-2100 transmission electron microscope. Elemental analyses for Mg, Ni, Al, and Co were performed with a Shimadzu ICPS-7500 inductively coupled plasma spectroscopy (ICP) instrument on solutions prepared by dissolving the powders scraped from the films in dilute HNO<sub>3</sub> (1:1). Conversion was detected on a Shimadzu 2010 GC-MS instrument using an HP5790 series mass-selective detector with a silicone capillary column (DB-5, poly(5% diphenyl–95% dimethylsiloxane, 25 m × 0.2 mm, 0.33  $\mu$ m film thickness). The specific surface area determination, pore volume, and size analysis were performed by BET and BJH methods using a Micromeritics ACAP 2020 analyzer. Prior to the measurements, samples were degassed at 200 °C for 6 h.

CO<sub>2</sub>-TPD of the catalysts was conducted on a TPDR0 110 series of Thermo. Before analysis, catalysts were heated to 500 °C for 4 h to remove interference gases adsorbed on the catalyst surface. Catalysts (100 mg) were treated in N<sub>2</sub> at 500 °C for 1 h and exposed to a CO<sub>2</sub> stream at room temperature until a saturation coverage was obtained. Weakly adsorbed CO<sub>2</sub> was removed by flushing with He at 100 °C for 0.5 h. The temperature was then increased at a linear rate of 5 °C/min from 80 °C to 500 °C.

The XPS measurements were carried out with a V. G. Scientific ESCALAB Mark II system. Mg K $\alpha$  ( $h\nu$  = 1253.6 eV) was used as X-ray source. The base pressure in the apparatus was about 2 × 10<sup>-6</sup> Pa during analysis. The binding energies (BE) were referenced to the C 1s peak (atmospheric contamination) at 284.6 eV. This reference gives BE values with an accuracy of  $\pm$ 0.1 eV. The experimental bands were fitted with a combination of Gaussian–Lorentzian lines using a linear baseline.

## 3. RESULTS AND DISCUSSION

**3.1. Structural and Morphological Study of the Structured Catalyst.** Figure 1 illustrates the XRD patterns

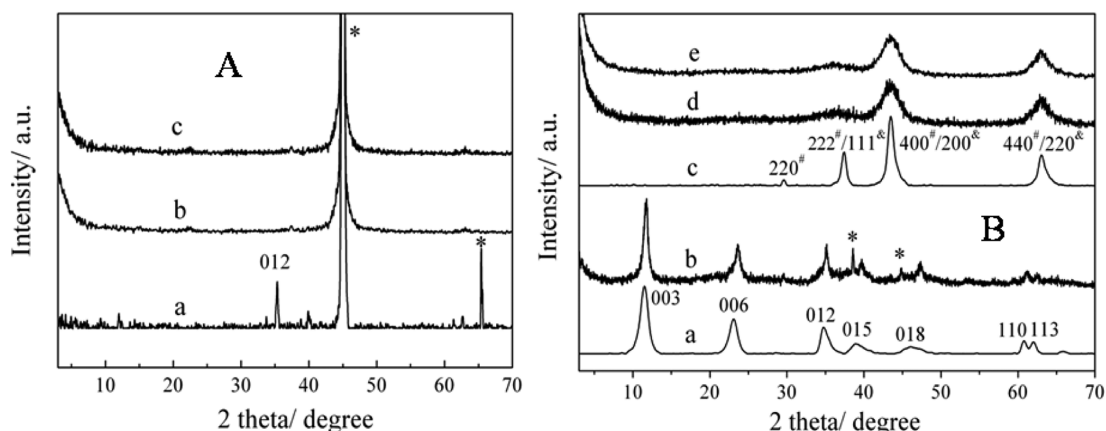


**Figure 1.** (A) XRD patterns of the (a) MgNiAl-LDH film, (b) MgNiAl-MMO film, and (c) CoPcS/MgNiAl-MMO film. (B) XRD patterns of (a) the powdered sample of MgNiAl-LDH, (b) the sample scraped from the MgNiAl-LDH film, (c) the powdered sample of MgNiAl-MMO, (d) the sample scraped from the MgNiAl-MMO film, and (e) the sample scraped from the CoPcS/MgNiAl-MMO film. The asterisk symbol indicates reflections from the Al substrate. The symbols # and & stand for NiO and MgO phase, respectively.

of the MgNiAl-LDH film, MgNiAl-MMO film, and CoPcS/MgNiAl-MMO film as well as the corresponding powdered samples scraped from the film for comparison. A weak reflection was observed at  $2\theta$   $35.0^\circ$  for the sample of MgNiAl-LDH film (Figure 1A-a), which can be attributed to the [012] reflection of the LDH phase; two strong reflections (denoted with asterisk) appear corresponding to the Al substrate. However, the powdered material scraped from the LDH film (Figure 1B-b) exhibits a series of characteristic LDH reflections ([003], [006], [012], [110], and [113]), in accordance with an LDH phase (Figure 1B-a), demonstrating the formation of MgNiAl-LDH film on the Al substrate. The characteristic [012] reflection as well as the absence of [001] reflections in Figure 1A-a are indicative of well-oriented LDH crystallites with their *ab* plane perpendicular to the substrate. In the case of the MMO film obtained by calcination of the LDH film (Figure 1A-b), only one reflection of the Al substrate was observed. However, the characteristic reflections belonging to crystalline NiO ([222], [400], [440]) (JCPDS 89-5881) and MgO ([111], [200], [220]) were detected for the powdered material scraped from the MMO film (Figure 1B-d), in accordance with the MgNiAl-MMO phase (Figure 1B-c). This indicates the occurrence of phase transformation from LDH to MMO. No obvious change can be found after loading CoPcS on the MMO film (Figure 1A-c); the scraped material (Figure 1B-e) also displays characteristic reflections similar to those in Figure 1B-d. Moreover, these results were further verified by TEM (Figure S2, Supporting Information). Therefore, it can be concluded that NiO and MgO phases were formed after calcination of the LDH film, and the subsequent loading of CoPcS did not change the structure of the MMO phase.

SEM images of the structured catalyst are shown in Figure 2. The MgNiAl-LDH film displays uniform hexagonal platelike microcrystals with a diameter of 1.0–1.4  $\mu\text{m}$  (Figure 2A and 2B) and a platelet thickness of 20–25 nm (Figure S3-A, Supporting Information), whose *ab*-plane is perpendicular to the substrate. This is consistent with the XRD results in Figure 1. The MMO film resulting from calcination of the LDH film inherits the original hexagonal morphology of the LDH precursor (Figure 2C and 2D), and a little shrinking in the size of hexagonal microcrystals (0.8–1.2  $\mu\text{m}$  in diameter and 20–25 nm in thickness, Figure S3-B, Supporting Information) compared with the parent LDH was observed. After CoPcS

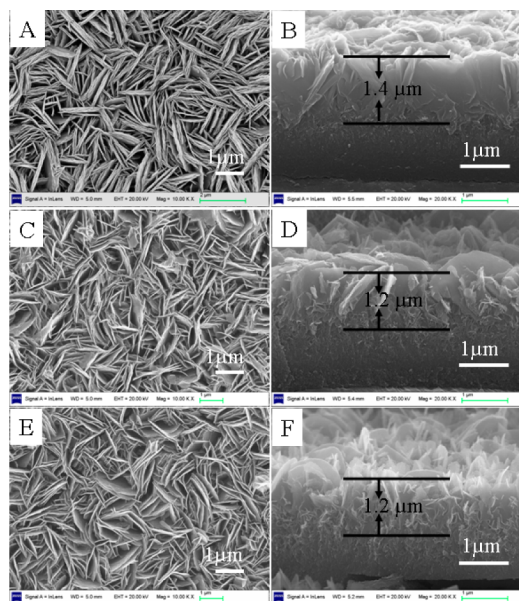


**Figure 2.** SEM images for the top-view and side-view of the MgNiAl-LDH film (A, B), MgNiAl-MMO film (C, D), and CoPcS/MgNiAl-MMO film (E, F).

(Figure 2E and 2F) was loaded, no significant change in the morphology of the CoPcS/MgNiAl-MMO film was observed in comparison with the MgNiAl-MMO film. The adhesion test shows that no significant peeling of the CoPcS/MgNiAl-MMO layer was found after cross-cutting through the film (Figure S4, Supporting Information), indicating a strong adhesion of the CoPcS/MgNiAl-MMO film to the substrate.

**3.2. Preparation of the Structured Catalysts for the Oxidation of Mercaptans. Influence of the Mg/Ni Ratio.** It was found that a different Mg/Ni ratio leads to a morphological variation of the MgNiAl-LDH film (Figure S5, Supporting Information). To study the effect of Mg/Ni ratio on the resulting catalytic behavior for the mercaptan oxidation, MgNiAl-LDH films with various Mg/Ni ratios (0.16, 0.42, 0.68, 1.16, 1.92, and 2.51, respectively) were therefore prepared, whose SEM images are shown in Figure 3. The size of the LDH microcrystals becomes larger and the stacking is more compact as the Mg/Ni ratio is increased over the entire

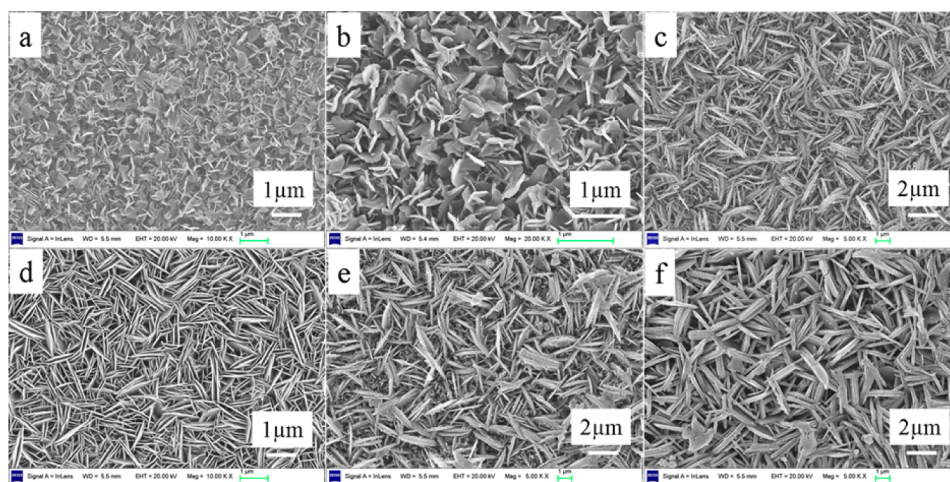


**Figure 3.** SEM images for the MgNiAl-LDH films with various Mg/Ni ratios (from a to f:  $r = 0.16, 0.42, 0.68, 1.16, 1.92, 2.51$ , respectively).

**Table 1.** Chemical Compositions of the LDH Film Precursors Prepared with Various Mg/Ni Ratios and the Corresponding Parameters of the Resulting Structured Catalysts (reaction time: 4 h)

Mg/Ni ratio	chemical composition of LDH sample	MMO (mg)	CoPcS (mg)	conversion (%)
0.16	$\text{Mg}_{0.116}\text{Ni}_{0.719}\text{Al}_{0.165}(\text{OH})_2(\text{CO}_3)_{0.0825} \cdot 0.41\text{H}_2\text{O}$	28.79	1.271	49.4
0.42	$\text{Mg}_{0.255}\text{Ni}_{0.603}\text{Al}_{0.142}(\text{OH})_2(\text{CO}_3)_{0.071} \cdot 0.48\text{H}_2\text{O}$	29.55	1.256	58.1
0.68	$\text{Mg}_{0.315}\text{Ni}_{0.465}\text{Al}_{0.220}(\text{OH})_2(\text{CO}_3)_{0.110} \cdot 0.53\text{H}_2\text{O}$	30.87	1.154	67.6
1.16	$\text{Mg}_{0.368}\text{Ni}_{0.318}\text{Al}_{0.314}(\text{OH})_2(\text{CO}_3)_{0.157} \cdot 0.46\text{H}_2\text{O}$	30.54	1.072	92.8
1.92	$\text{Mg}_{0.463}\text{Ni}_{0.241}\text{Al}_{0.296}(\text{OH})_2(\text{CO}_3)_{0.148} \cdot 0.55\text{H}_2\text{O}$	31.92	1.045	82.7
2.53	$\text{Mg}_{0.513}\text{Ni}_{0.203}\text{Al}_{0.284}(\text{OH})_2(\text{CO}_3)_{0.142} \cdot 0.44\text{H}_2\text{O}$	33.17	1.069	88.1

range. Moreover, the thickness of single LDH microcrystals first increases as the Mg/Ni ratio rises from 0.16 to 1.16 and then decreases with a further increase in the Mg/Ni ratio in the range 1.16–2.51 (Figure S6, Supporting Information).

Structured catalysts were prepared by calcination of the LDH films mentioned above and then immersing them into CoPcS methanol solution (30 ppm) for 1 h, which are represented as CoPcS/MMO- $r$  ( $r$  denotes the Mg/Ni ratio of LDH film precursor). Table 1 lists the chemical composition of the LDH film precursor and the corresponding parameters of the structured catalysts, from which the content of MMO increases with the increase in  $r$ , while the content of CoPcS decreases. Catalytic activity evaluation of the CoPcS/MMO- $r$  ( $r = 0.16, 0.42, 0.68, 1.16, 1.92$ , and  $2.53$ ) structured catalysts for the oxidation of mercaptan was performed, and the results are shown in Figure 4. The catalytic conversion increases at first to a maximum and then decreases with the increase in Mg/Ni ratio (reaction time: 4 h). The CoPcS/MMO catalyst ( $r = 1.16$ , curve d) exhibits the highest conversion of mercaptan (92.8%, 4 h) compared with the other samples (curves a, b, c, e, and f), as a result of the lowest deactivation. The results indicate that the Mg/Ni ratio plays an important role in the morphology and the resulting conversion over the structured catalyst, which will be discussed in the next section.

**Influence of the Loading Amount of CoPcS.** The loading amount of CoPcS plays an important role for the structured catalyst. A lower CoPcS loading results in less active sites for the catalyst (Co atom in CoPcS), which decreases the conversion of mercaptan, while a larger loading would lead to the aggregation of CoPcS and resulting deactivation. Therefore, an appropriate CoPcS loading (a rational ratio of CoPcS to basic site) is beneficial to enhance the synergistic effect between CoPcS and basic site, which improves the catalytic behavior.

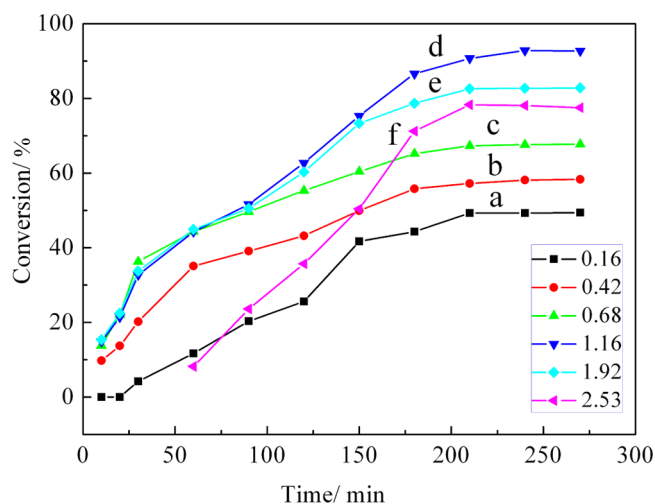


**Figure 4.** Catalytic conversion of 1-octanethiol over the CoPcS/MMO- $r$  structured catalysts with various Mg/Ni ratios at room temperature and atmospheric pressure (from a to f:  $r = 0.16, 0.42, 0.68, 1.16, 1.92, 2.53$ , respectively).

Structured catalysts represented as CoPcS/MMO- $c$  ( $c$  stands for the concentration of CoPcS methanol solution) were prepared by immersing the MMO film into CoPcS methanol solution with various concentrations ( $c = 10, 20, 30$ , and  $40$  ppm, respectively) for 1 h. An increase in the CoPcS content of these catalysts along with the increase in concentration was found based on the results of elemental analysis (Table 2), and their catalytic behavior for the oxidation of mercaptan is shown in Figure 5. The conversion of mercaptan increases at first to a maximum and then decreases along with the increase in CoPcS concentration (Table 2). The CoPcS/MMO catalyst ( $c = 30$

**Table 2. Catalytic Conversion of the Structured Catalysts with Various CoPcS Loadings (area of the structured catalyst: 140 cm<sup>2</sup>; reaction time: 4 h)**

CoPcS concentration in methanol (ppm)	MMO (mg)	CoPcS (mg)	conversion (%)
10	30.54	0.787	74.9
20	30.54	0.923	79.3
30	30.54	1.072	92.8
40	30.54	1.263	85.2

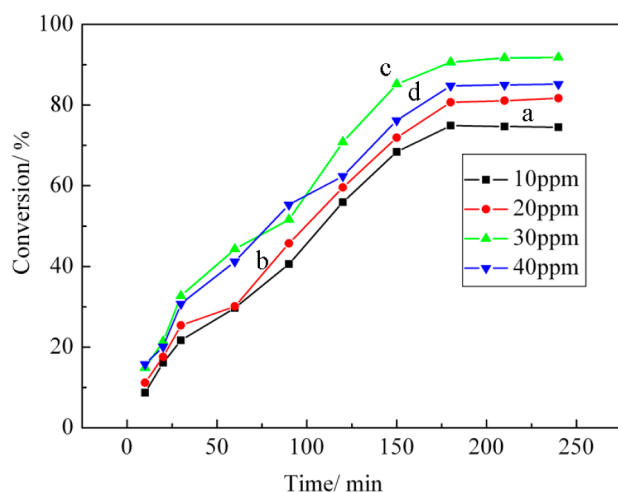


**Figure 5.** Catalytic conversion of 1-octanethiol over the CoPcS/MMO-*c* structured catalysts at room temperature and atmospheric pressure (from a to d: *c* = 10, 20, 30, 40 ppm, respectively).

ppm) displays the highest conversion (92.8%) among these structured catalysts. The gradual increase in the maximum conversion of CoPcS/MMO (*c* = 10, 20, and 30 ppm) is attributed to the increase in CoPcS content, while a further increase (*c* = 40 ppm) may lead to the aggregation of CoPcS and the resulting deactivation of the structured catalyst (CoPcS/MMO-40). Therefore, *c* = 30 ppm was chosen for further study.

**3.3. Catalytic Oxidation of Mercaptan with Different Catalysts.** The catalytic performance of the CoPcS/MgNiAl-MMO structured catalyst for the oxidation of mercaptan was studied, as well as the CoPcS/Al film, CoPcS/MgAl-MMO film, CoPcS/NiAl-MMO film, and CoPcS/MgNiAl-MMO powdered sample for comparison. The catalytic conversion of these catalysts was tested (Figure 6), and the results are listed in Table 3. No conversion was observed for the CoPcS/Al sample; the CoPcS/NiAl-MMO catalysts (both film and powder) show rather low conversion levels, i.e., 20.1% (film) and 8.2% (powder), probably owing to its unsuitable basicity. In our previous work,<sup>23</sup> a CoPcS/MgAl-MMO film catalyst with a catalytic conversion (85.7%) for mercaptan oxidation higher than that of its powdered analogue (38.5%) was confirmed. In this work, the CoPcS/MgNiAl-MMO film catalyst shows the highest conversion (92.8%), much higher than that of CoPcS/MgNiAl-MMO powdered catalyst (60.1%) and markedly superior to that of the CoPcS/MgAl-MMO and CoPcS/NiAl-MMO film catalysts. On the basis of the results above, it is proposed that an enhanced synergistic effect between active CoPcS and basicity of MgNiAl-MMO was obtained in this work, which accounts for the largely enhanced catalytic activity and will be discussed in the next section.

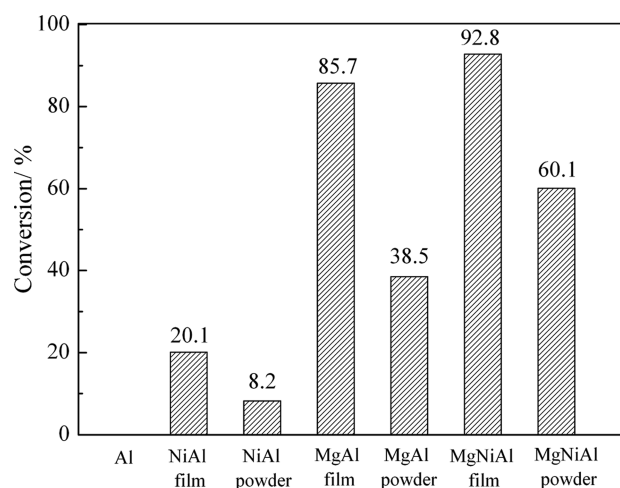


**Figure 6.** Conversion of mercaptan with the presence of various catalysts running for 4 h.

### 3.4. Physicochemical Properties of the Structured Catalyst.

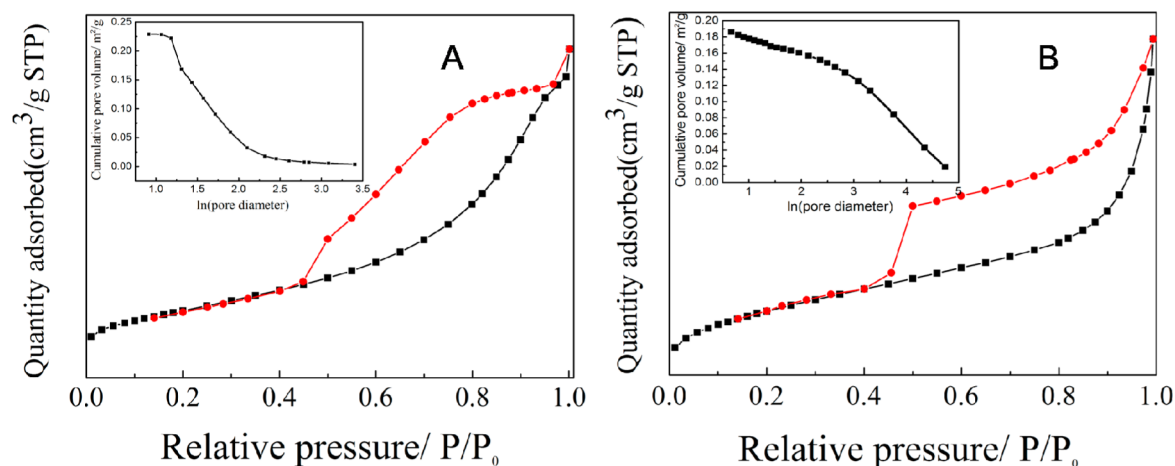
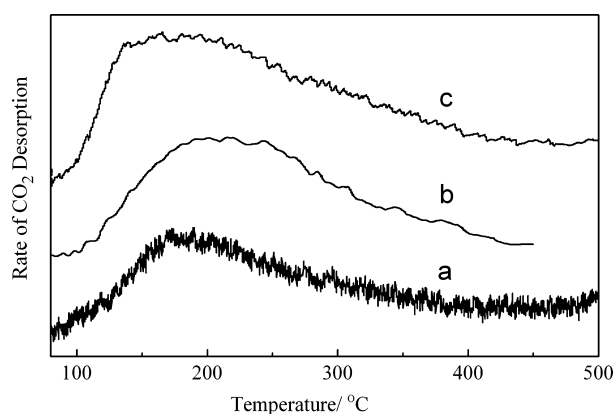
Figure 7 shows the N<sub>2</sub> adsorption–desorption isotherms and pore size distribution curves for the CoPcS/MgNiAl-MMO powdered and film catalysts, and the specific surface areas are summarized in Table 1. Both samples exhibit an intermediate isotherm between type II (absence of a plateau at high *p/p*<sub>0</sub>) and type IV adsorption (little N<sub>2</sub> adsorption at lower *p/p*<sub>0</sub>) according to Groen's report.<sup>24,25</sup> The adsorption isotherm of these samples slowly increases with the increase in *p/p*<sub>0</sub> at lower relative pressure while a rapid increase in adsorption isotherm was observed at higher *p/p*<sub>0</sub>; a saturation adsorption was not observed even at the saturation vapor pressure, indicating the existence of mesoporous or macropores.<sup>26</sup> This is further confirmed by the corresponding wide distribution of pore size, which derived from the adsorption branch owing to the existence of the tensile strength effect (TSE)<sup>24</sup> in the desorption isotherm of film samples. An H3-type hysteresis loop was observed for CoPcS/MgNiAl-MMO powdered sample (Figure 7A), which indicates the presence of slit-shaped pores. In the case of the CoPcS/MgNiAl-MMO film sample (Figure 7B), a mixture of H2–H3 hysteresis loops was observed, indicating the presence of slit-shaped and ink-bottle pores in the whole mesopore network.<sup>24,25</sup> The pore size distribution for the CoPcS/MgNiAl-MMO film sample (10–100 nm) is attributed to the homogeneous morphology of MMO microcrystals and their oriented stacking on the substrate. In addition, the catalytic evaluation shows that the specific surface area of the LDH film catalyst is not a key factor in determining its activity, while the enhancement of the synergistic effect between the oxidation center (CoPcS) and the moderate basic site is more crucial.

Taking into account the crucial role of catalyst basicity in the oxidation of mercaptan, we recorded CO<sub>2</sub>-TPD profiles to reveal the difference in the strength and number of basic sites for these catalysts, as shown in Figure 8, and Figure S7, Supporting Information. Our previous work<sup>23</sup> confirms that the CoPcS/MgAl-MMO powdered catalyst provides three species of basic sites (weak, moderate, and strong basic site; Figure S7a, Supporting Information), and the moderate basic site plays a key role in the catalytic activity. For the CoPcS/MgAl-MMO and CoPcS/NiAl-MMO film catalysts, the peak at 170 °C and 200 °C is observed, respectively, which is attributed to the moderate basic site (Figure 8a). The stronger basicity of NiAl-

**Table 3.** Chemical Composition, BET Specific Surface Area, Basicity, and Mercaptan Conversion for Various Catalysts (reaction time: 4 h)

catalyst	(Ni+Mg)/Al ratio	CoPcS (mg)	MMO (mg)	SBET (m <sup>2</sup> /g)	adsorbed CO <sub>2</sub> (mmol/g)	moderate basic site (mmol/g)	conversion (%)
CoPcS/Al		0.28					0.0
CoPcS/NiAl-film	2.47	1.31	37.8	17.9	0.33	0.33	20.1
CoPcS/NiAl-powder	2.23	1.39	37.8	30.4	0.39	0.12	8.2
CoPcS/MgAl -film <sup>a</sup>	2.13	1.00	32.9	15.5	0.31	0.31	85.7
CoPcS/MgAl-powder <sup>a</sup>	2.11	1.12	32.9	269.2	0.44	0.20	38.5
CoPcS/MgNiAl-film	2.18	1.07	30.54	97.7	0.49	0.49	92.8
CoPcS/MgNiAl-powder	2.12	1.26	30.54	118.9	0.38	0.38	60.1

<sup>a</sup>Datum derived from our previous work (ref 23).

**Figure 7.** Nitrogen adsorption–desorption isotherms and corresponding pore size distribution curves (inset) of CoPcS/MgNiAl-MMO powdered (A) and film (B) sample.**Figure 8.** TPD profiles of CO<sub>2</sub> on the (a) CoPcS/MgAl-MMO film, (b) CoPcS/NiAl-MMO film, and (c) CoPcS/MgNiAl-MMO film sample.

MMO relative to the MgAl-MMO film is rather unusual, which is possibly related to the unique preparation method (in situ growth followed by calcination). The NiAl powdered catalyst (Figure S7b, Supporting Information) displays two species of basic sites, i.e., moderate (~165 °C) and strong basic site (~390 °C), while the moderate basic site (~205 °C) is predominant in the film catalyst (Figure 8b). For the MgNiAl catalysts, the maximum desorption rate of CO<sub>2</sub> appears at ~206 °C for the powdered sample (Figure S7c, Supporting Information) and ~163 °C for the film sample (Figure 8c), respectively, corresponding to the moderate basic site. A comparison study among the three film catalysts reveals that

the MgNiAl film sample shows a ~7 °C and ~37 °C lower temperature in the moderate basic peak in comparison with MgAl and NiAl film sample, respectively. This indicates that the MgNiAl film sample presents more mild basicity, accounting for its highest catalytic activity. In addition, the percentage and number of CO<sub>2</sub> adsorbed on each basic site were calculated by integration, and the results show the MgNiAl film catalyst possesses the largest number of moderate basic sites (0.49 mmol/g) among these catalysts (Table 3). Although the CoPcS/NiAl-MMO and CoPcS/MgAl-MMO film catalysts show very close numbers of moderate basic sites (0.33 and 0.31 mmol/g, respectively), the former catalyst displays a much higher conversion toward the oxidation of mercaptan. A possible reason is that the moderate basicity of NiAl-MMO is not suitable in this reaction, which has been reported by other researchers,<sup>27</sup> while the moderate basic sites derived from MgAl-MMO are beneficial to the oxidation of mercaptan.<sup>28</sup> However, a synergistic effect between Mg and Ni was found in this work: the CoPcS/MgNiAl-MMO film catalyst shows a significant increase in moderate basic sites and the highest conversion. The intrinsic mechanism of synergistic effect is expected to be rather complicated, which is under investigation in our lab.

For further investigation of the basicity of structured catalysts, X-ray photoelectron spectroscopy (XPS) was performed. Figure 9 shows the XPS spectra of O1s for MgAl, NiAl, and MgNiAl-LDH precursor and the resulting CoPcS/MMO catalysts. One broad peak at 530–534 eV was found for the LDH precursors (Figure 9, curve a), which is assigned to surface hydroxyl and carbonate groups (O<sub>a</sub>).<sup>29</sup> However, the

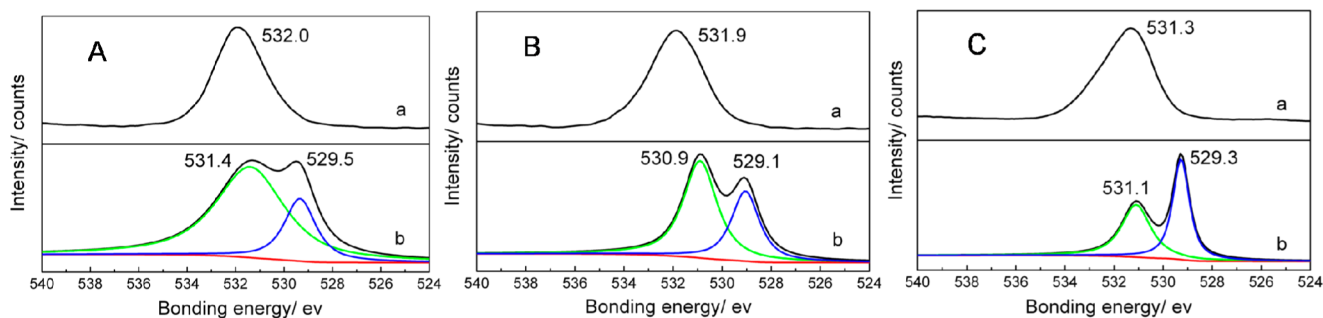


**Figure 9.** XPS of O1s for (A) MgAl, (B) NiAl, and (C) MgNiAl systems: (a) the LDH precursor, (b) the corresponding CoPcS/MMO catalyst.

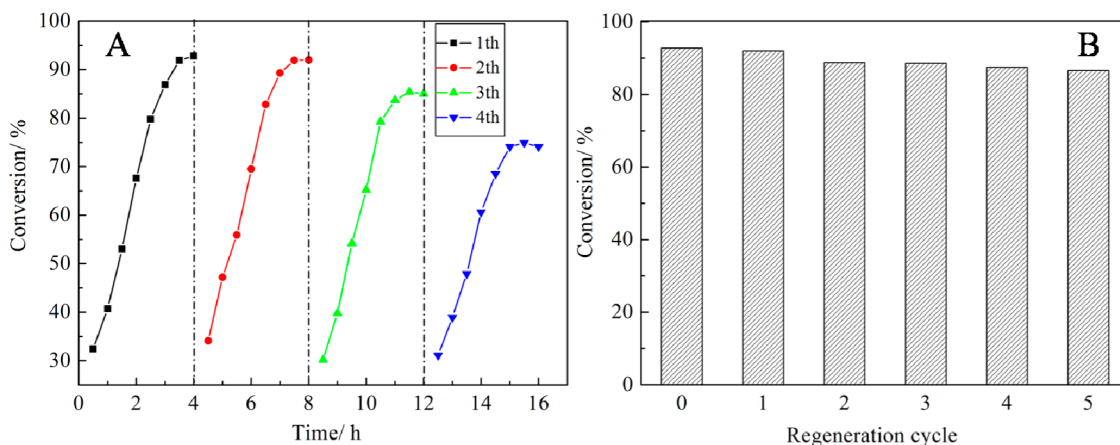


**Figure 10.** (A) The catalytic capability of the CoPcS/MgNiAl-MMO film catalyst for the oxidation of mercaptan. (B) The conversion of mercaptan vs regeneration cycle. Reaction time: 4 h.

XPS spectra of O1s for the CoPcS/MMO film catalysts including MgAl, NiAl, and MgNiAl show doublet peaks at 530–534 eV and 528–530 eV (Figure 9, curve b). The former peak corresponds to oxygen species of surface hydroxyl or carbonate groups, while the latter one is attributed to lattice oxygen ( $O_{\beta}$ ),<sup>30</sup> indicating the formation of metal oxide by calcination of LDH precursors. This is in accordance with the results of TEM images (Figure S2, Supporting Information). It was reported that the lattice oxygen ( $O_{\beta}$ ) accounts for the basicity of structured catalysts.<sup>15</sup> The relative ratio between  $O_{\beta}$  and  $O_{\alpha}$  for different structured catalysts was calculated by integration, and the results reveal that the  $O_{\beta}/O_{\alpha}$  value for the MgNiAl structured catalyst (1.10) is much larger than that of the MgAl (0.60) and NiAl (0.32) ones. This indicates that more basic sites were formed in the MgNiAl catalyst than in the MgAl or NiAl one in the calcination process. This agrees well with the results of  $CO_2$ -TPD that the MgNiAl structured catalyst shows the maximum moderate basic sites (0.49 mmol/g) among all these catalysts (Table 3). Consequently, it can be concluded that an enhanced synergistic effect between the oxidation center (CoPcS) and the abundant moderate basic sites in the CoPcS/MgNiAl-MMO structured catalyst is responsible for its excellent catalytic activity.

**3.5. Regeneration of the Structured Catalysts.** Because the time to regenerate the catalysts is very essential for practical application, the lifetime and regeneration of the CoPcS/MgNiAl-MMO structured catalyst were examined. Figure 10A shows the catalytic lifetime of the structured catalyst through four cycles. The conversion of mercaptan decreased gradually (from 92.8% to 85.4%) in the first three cycles; an obvious decrease in conversion (74.9%) was observed in the fourth

cycle (curve d), indicating the inactivity of the structured catalyst. The catalyst deactivation is caused mainly by the coverage of active sites with gumlike compounds in the oil (as shown in Figure 11). Therefore, removal of the surface-

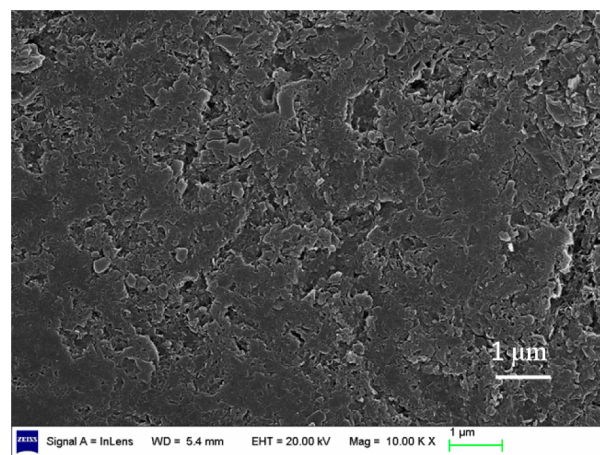


**Figure 11.** SEM image of the structured catalyst used.

adsorbed impurity is necessary in the regeneration process to allow reuse. The regeneration of the structured catalyst was performed by washing with acetone–dimethyl sulfoxide solvent (1:1, v/v) followed by calcination (at 500 °C) and loading CoPcS. The consecutive catalysis–regeneration cycles of the structured catalyst were carried out five times, and the results are shown in Figure 10B. No significant decrease in the conversion of mercaptan was observed even in the fifth cycle.

Moreover, the structure and morphology of the CoPcS/MgNiAl-MMO film catalyst remained unchanged after five catalysis–regeneration cycles, which was revealed by XRD and SEM (Figure S8, Supporting Information). In addition, the regeneration lifetime and cycles of the powdered catalyst were performed for comparison (Figure S9, Supporting Information). A short regeneration lifetime was observed (Figure S9-A, Supporting Information), and only 35.3% of conversion was maintained after the second regeneration cycle (Figure S9-B, Supporting Information), owing to the leaching of CoPcS and/or the aggregation of the powdered sample. The results above indicate that the structured catalyst exhibits high catalytic activity, stability, and regeneration ability and is a promising catalyst for the sweetening process. The deactivation mechanism of the catalyst and its regeneration process should be further studied and explored to achieve commercial scale application.

#### 4. CONCLUSION

A structured catalyst based on CoPcS supported on MgNiAl-MMO film was fabricated, which shows high catalytic activity, stability, and good recyclability for the mercaptan sweetening process. The structured catalyst is composed of thin MMO nanoflakes perpendicular to the Al substrate with desirable mechanical strength and high adhesion to the substrate. XPS spectra and CO<sub>2</sub>-TPD revealed that the basicity and number of moderate basic sites for the MgNiAl structured catalyst can be modulated conveniently by changing the relative content of Mg and Ni. The structured catalyst CoPcS/MgNiAl-MMO exhibits the highest conversion reached in the 4 h run compared with CoPcS/MgAl-MMO and CoPcS/NiAl-MMO catalysts, which is attributed to the enhanced synergistic effect between the oxidation center (CoPcS) and the moderate basic sites. The regeneration and recycle usage of the structured catalyst were also demonstrated. Therefore, the structured catalyst in this work exhibits the advantages of high catalytic activity and stability, good recyclability, and convenient manipulation. It is expected that the MgNiAl structured catalyst could be potentially used as an eco-friendly catalyst for the sweetening process in the oil refining industry.

#### ■ ASSOCIATED CONTENT

##### Supporting Information

Photograph (Figure S1), TEM (Figure S2), SEM images (Figures S3–S6), CO<sub>2</sub>-TPD (Figure S7), XRD (Figure S8), regeneration cycle (Figure S9). This material is available free of charge via the Internet at <http://pubs.acs.org>.

#### ■ AUTHOR INFORMATION

##### Corresponding Authors

\*Phone: +86-10-64412131. Fax: +86-10-64425385. E-mail: [weimin@mail.buct.edu.cn](mailto:weimin@mail.buct.edu.cn).

\*E-mail: [wanglr@mail.buct.edu.cn](mailto:wanglr@mail.buct.edu.cn).

##### Notes

The authors declare no competing financial interest.

#### ■ ACKNOWLEDGMENTS

This work was supported by the 973 Program (grant no. 2011CBA00504), the National Natural Science Foundation of China (NSFC), the Scientific Fund from Beijing Municipal Commission of Education (20111001002), and the Fundamental Research Funds for the Central Universities (ZD 1303).

M. Wei particularly appreciates the financial aid from the China National Funds for Distinguished Young Scientists of the NSFC.

#### ■ REFERENCES

- (1) He, J.; Liu, X.; Li, L.; Wang, B.; Hu, J. Experimental Investigation of the Interaction of Dimethyl Sulfide/Ethyl Mercaptan with Nanomanganese Dioxide. *Ind. Eng. Chem. Res.* **2012**, *51*, 15912.
- (2) Bedell, S. A.; Miller, M. Aqueous Amines as Reactive Solvents for Mercaptan Removal. *Ind. Eng. Chem. Res.* **2007**, *46*, 3729.
- (3) Petre, C. F.; Larachi, F. Removal of Methyl Mercaptide by Iron/Cerium Oxide-Hydroxide in Anoxic and Oxidic Alkaline Media. *Ind. Eng. Chem. Res.* **2007**, *46*, 1990.
- (4) Das, G.; Sain, B.; Kumar, S.; Garg, M. O.; MuraliDhar, G. Synthesis, Characterization and Catalytic Activity of Cobalt Phthalocyanine Tetrasulphonamide in Sweetening of LPG. *Catal. Today* **2009**, *141*, 152.
- (5) Wallace, T.; Schriesheim, A.; Hurwitz, H.; Glaster, M. Base Catalyzed Oxidation of Mercaptans in the Presence of Inorganic Transition Metal Complexes. *Ind. Eng. Chem. Process Des. Dev.* **1964**, *3*, 237.
- (6) Alcaraz, J. J.; Arena, B. J.; Gillespie, R. D.; Holmgren, J. S. Solid Base Catalysts for Mercaptan Oxidation. *Catal. Today* **1998**, *43*, 89.
- (7) Guo, X.; Zhang, F.; Xu, S.; Cui, Z.; Evans, D. G.; Duan, X. Effects of Varying the Preparation Conditions on the Dielectric Constant of Mixed Metal Oxide Films Derived from Layered Double Hydroxide Precursor Films. *Ind. Eng. Chem. Res.* **2009**, *48*, 10864.
- (8) Fogg, A. M.; Green, V. M.; Harvey, H. G.; O'Hare, D. New Separation Science Using Shape-Selective Ion Exchange Intercalation Chemistry. *Adv. Mater.* **1999**, *11*, 1466.
- (9) Fogg, A. M.; Dunn, J. S.; Shyu, S. G.; Cary, D. R.; O'Hare, D. Selective Ion-Exchange Intercalation of Isomeric Dicarboxylate Anions into the Layered Double Hydroxide [LiAl<sub>2</sub>(OH)<sub>6</sub>]Cl·H<sub>2</sub>O. *Chem. Mater.* **1998**, *10*, 351.
- (10) Gursky, J. A.; Blough, S. D.; Luna, C.; Gomez, C.; Luevano, A. N.; Gardner, E. A. Particle-Particle Interactions between Layered Double Hydroxide Nanoparticles. *J. Am. Chem. Soc.* **2006**, *128*, 8376.
- (11) He, S.; Zhao, Y.; Wei, M.; Duan, X. Preparation of Oriented Layered Double Hydroxide Film Using Electrophoretic Deposition and Its Application in Water Treatment. *Ind. Eng. Chem. Res.* **2011**, *50*, 2800.
- (12) Wei, M.; Zhang, X.; Evans, D. G.; Duan, X. Rh-TPPTS Intercalated Layered Double Hydroxides as Hydroformylation Catalyst. *AIChE J.* **2007**, *53*, 2916.
- (13) Chatti, I.; Ghorbel, A.; Grange, P.; Colin, J. M. Oxidation of Mercaptans in Light Oil Sweetening by Cobalt(II) Phthalocyanine-Hydroxide Catalysts. *Catal. Today* **2002**, *75*, 113.
- (14) Di Cosimo, J. I.; Diez, V. K.; Xu, M.; Iglesia, E.; Apesteguía, C. R. Structure and Surface and Catalytic Properties of Mg-Al Basic Oxides. *J. Catal.* **1998**, *178*, 499.
- (15) McKenzie, A. L.; Fishel, C. T.; Davis, R. J. Investigation of the Surface Structure and Basic Properties of Calcined Hydroxaltes. *J. Catal.* **1992**, *138*, 547.
- (16) Lei, X. D.; Zhang, F. Z.; Yang, L.; Guo, X. X.; Tian, Y. Y.; Fu, S. S.; Li, F.; Evans, D. G.; Duan, X. Highly Crystalline Activated Layered Double Hydroxides as Solid Acid-Base Catalysts. *AIChE J.* **2007**, *53*, 932.
- (17) Mitchell, S.; Biswick, T.; Jones, W.; Williams, G.; O'Hare, D. A Synchrotron Radiation Study of the Hydrothermal Synthesis of Layered Double Hydroxides from MgO and Al<sub>2</sub>O<sub>3</sub> Slurries. *Green Chem.* **2007**, *9*, 373.
- (18) Choudary, B. M.; Kantam, M. L.; Reddy, C. V.; Rao, K. K.; Figueras, F. Henry Reactions Catalysed by Modified Mg-Al Hydroxaltes: An Efficient Reusable Solid Base for Selective Synthesis of  $\beta$ -Nitroalkanol. *Green Chem.* **1999**, *1*, 187.
- (19) Valente, J. S.; Figueras, F.; Gravelle, M.; Kumbhar, P.; Lopez, J.; Besse, J. P. Basic Properties of the Mixed Oxides Obtained by Thermal

Decomposition of Hydrotalcites Containing Different Metallic Compositions. *J. Catal.* **2000**, *189*, 370.

(20) Díez, V. K.; Ferretti, C. A.; Torresi, P. A.; Apesteguía, C. R.; Di Cosimo, J. I. Effect of MgO Activation Conditions on Its Catalytic Properties for Base-Catalyzed Reactions. *Catal. Today* **2011**, *173*, 21.

(21) Bezen, M. C. I.; Breitkopf, C.; Lercher, J. A. Influence of Fluoride Anions on the Acid–Base Properties of Mg/Al Mixed Oxides. *ACS Catal.* **2011**, *1*, 1384.

(22) Liu, H.; Yang, X.; Ran, G.; Min, E. Bifunctional Catalysts of Supported Cobalt-Phthalocyanine with Oppositively Charged Ions for Autoxidation of Mercaptan. *Acta Phys.-Chim. Sin.* **1999**, *15*, 918.

(23) Sun, Z. Y.; Jin, L.; He, S.; Zhao, Y. F.; Wei, M.; Evans, D. G.; Duan, X. A Structured Catalyst Based on Cobalt Phthalocyanine/Calcined Mg–Al Hydrotalcite Film for the Oxidation of Mercaptan. *Green Chem.* **2012**, *14*, 1909.

(24) Groen, J. C.; Peffer, L. A. A.; Pérez-Ramírez, J. Pore Size Determination in Modified Micro- and Mesoporous Materials. Pitfalls and Limitations in Gas Adsorption Data Analysis. *Microporous Mesoporous Mater.* **2003**, *60*, 1.

(25) Abelló, S.; Pérez-Ramírez, J. Steam Activation of Mg–Al Hydrotalcite. Influence on the Properties of the Derived Mixed Oxides. *Microporous Mesoporous Mater.* **2006**, *96*, 102.

(26) Zhao, Y. F.; Wei, M.; Lu, J.; Wang, Z. L.; Duan, X. Biotemplated Hierarchical Nanostructure of Layered Double Hydroxides with Improved Photocatalysis Performance. *ACS Nano* **2009**, *3*, 4009.

(27) Cairon, O.; Dumitriu, E.; Guimon, C. Acid–Basicity of Mg–Ni–Al Mixed Oxides from LDH Precursors: A FTIR and XPS Study. *J. Phys. Chem. C* **2007**, *111*, 8015.

(28) Liu, H.; Min, E. Catalytic Oxidation of Mercaptans by Bifunctional Catalysts Composed of Cobalt Phthalocyanine Supported on Mg–Al Hydrotalcite-Derived Solid Bases: Effects of Basicity. *Green Chem.* **2006**, *8*, 657.

(29) Wei, L. S.; Li, J. H.; Tang, X. F. NO<sub>x</sub> Storage at Low Temperature over MnO<sub>x</sub>–SnO<sub>2</sub> Binary Metal Oxide Prepared through Different Hydrothermal Process. *Catal. Lett.* **2009**, *127*, 107.

(30) Hamoudi, S.; Larachi, F.; Adnot, A.; Sayari, A. Characterization of Spent MnO<sub>2</sub>/CeO<sub>2</sub> Wet Oxidation Catalyst by TPO–MS, XPS, and S-SIMS. *J. Catal.* **1999**, *185*, 333.